Stanford
SCHOOL OF EARTH, ENERGY & ENVIRONMENTAL SCIENCES
Geophysics

# Integrating non-collocated well and geophysical data to capture lithological heterogeneity at a managed aquifer recharge and recovery site


Ian Gottschalk*[1], Thomas Hermans[2,1], Jef Caers[1], David Cameron[1], Rosemary Knight[1], Julia Regnery[3], John McCray[3]

1. Stanford University, Stanford, CA 2. University of Liege, Liege, Belgium 3. Colorado School of Mines, Golden, CO
*Corresponding author; email: *ianpg@stanford.edu*


## Introduction

Aquifer recharge and recovery (ARR) is the process of enhancing natural groundwater resources and recovering water for later use by constructing engineered conveyances—in our case by recharge ponds. Subsurface lithological heterogeneity can impair attempts at estimating **where** and **how quickly** water flows through the subsurface.

Here, we explore three separate methods for transforming geophysical data not collocated with borehole information into lithological data at an ARR site in order to understand the lithological heterogeneity which dictates flow. Each method is evaluated in a Bayesian framework for integration into lithology and flow models.

Figure 1: Aquifer recharge and recovery

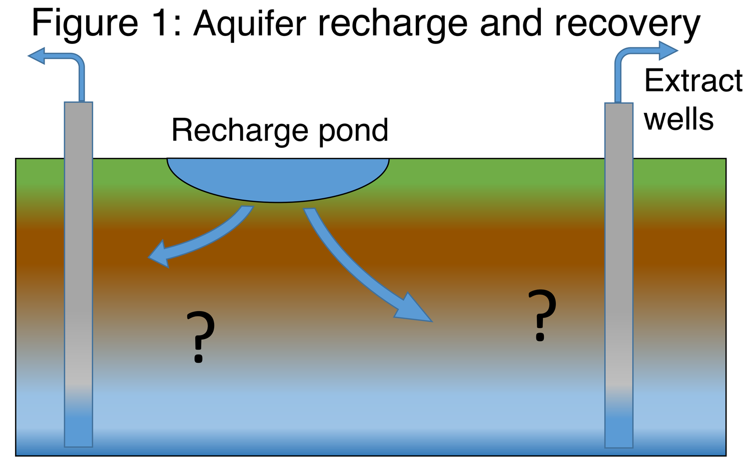


## Field Site

- Near Aurora, CO
- Geomorphological setting: unconsolidated fluvial sediments, with many thin clay fingers.
- 26 recovery wells (blue) around the perimeter, 75-170m apart.
- 25 electrical resistivity tomography (ERT) profiles were collected in and near the central and southwestern recharge basins.
- ERT measurements are not collocated with the wells in the area

Figure 2: Field site and ERT profiles

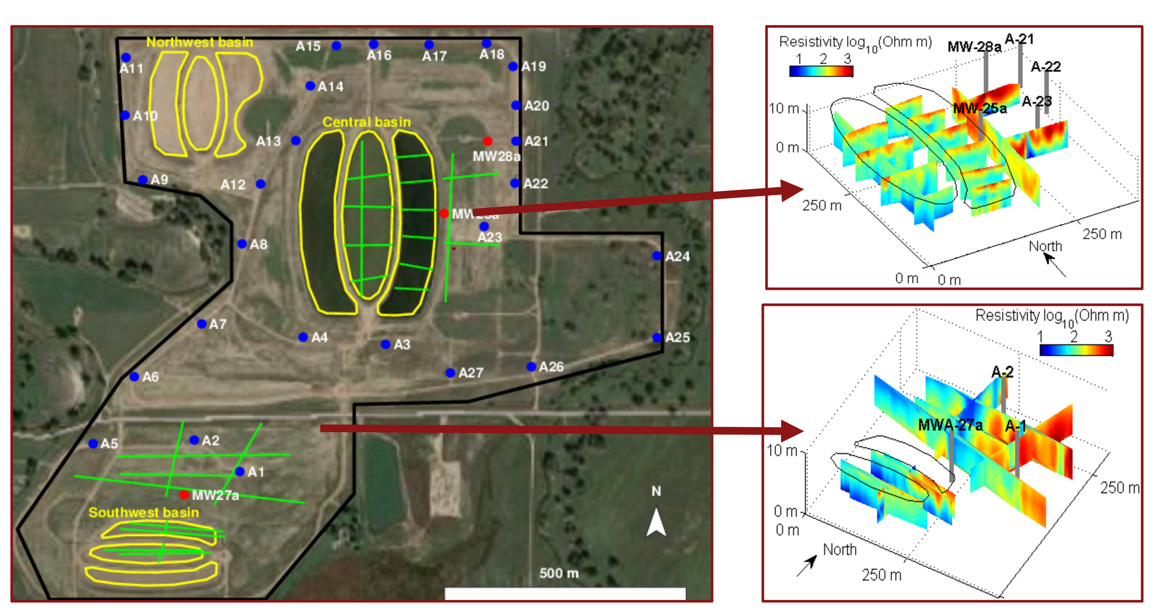

## Resistivity-lithology transform

The transformation from resistivity to lithology contains significant uncertainty, which is amplified when geological data is not collocated with geophysical data, because of variation with spatial displacement. Few guidelines exist for the commonly encountered case where geological and geophysical information are not collocated (for coincidental or logistical reasons).

In this study, we transform resistivity to lithology using a Bayesian framework, according to:

$$Prob(\phi_i|\rho) = \frac{Prob(\phi_i) * Prob(\rho|\phi_i)}{\sum_j Prob(\phi_j) * Prob(\rho|\phi_j)}$$

$\phi$: lithology or facies
$\rho$: resistivity measurements from ERT (ohm-m)

## Three methods

### 1. Search template

A search template was used to create an empirical probability distribution. The template takes a resistivity measurement from the ERT profile and pairs it to the nearest two borehole measurements of lithology, given a search template of 80m x 80m x 1ft.

Search criteria were imposed based on the assumption of horizontal deposition, which were supported by the horizontal variogram of well data.

Figure 3: Search template schematic

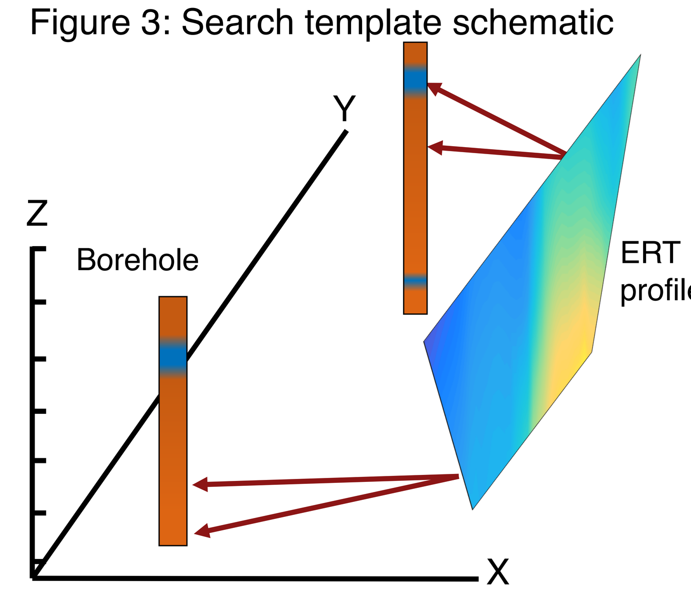


Figure 4: Search template histogram

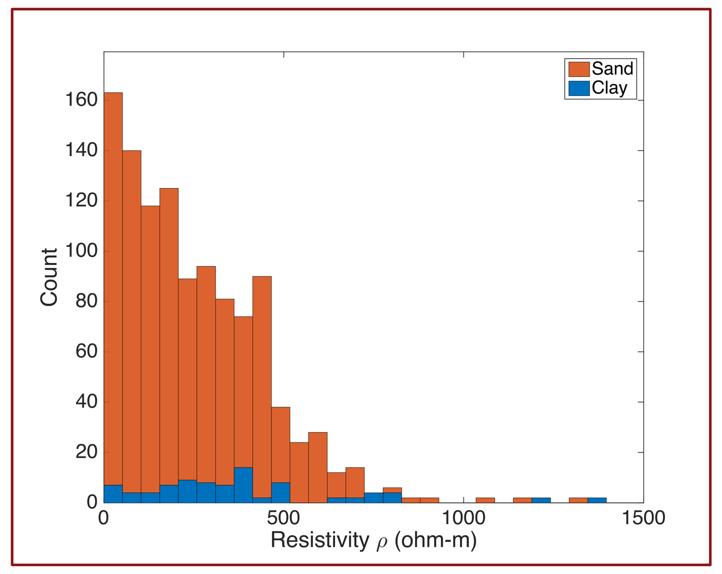


### 2. Maximum likelihood estimation of ERT histograms

The histograms of the 25 ERT profiles were fitted with a bimodal normal distribution. Each parameter was averaged throughout the 25 lines to create the governing probability density function, for use in Bayes' Theorem (Figure 6).

Final distribution statistics: $P_2$: 44.4%
$P_1$: 55.6% $\mu_2$: 234.3
$\mu_1$: 64.3 $\sigma_2$: 129.3
$\sigma_1$: 36.6

Figure 5: Histogram and PDF fit of each ERT profile

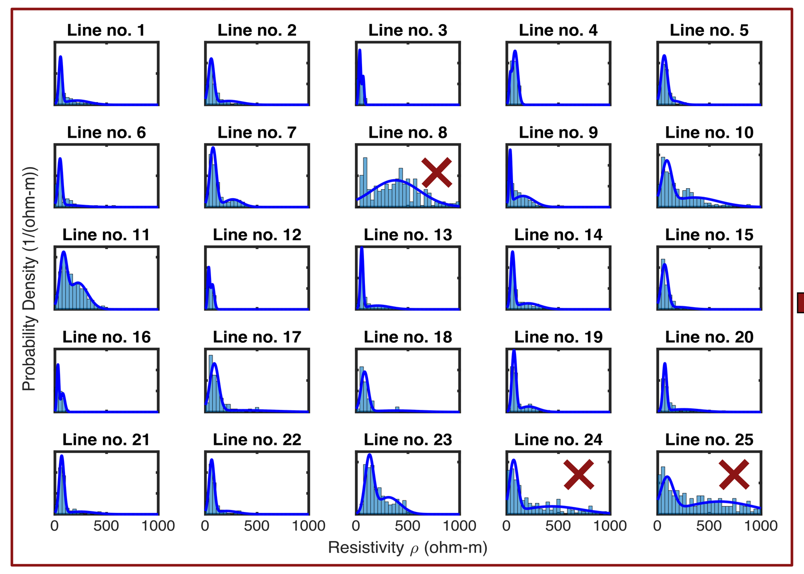


Figure 6: Combined PDF from all ERT profiles

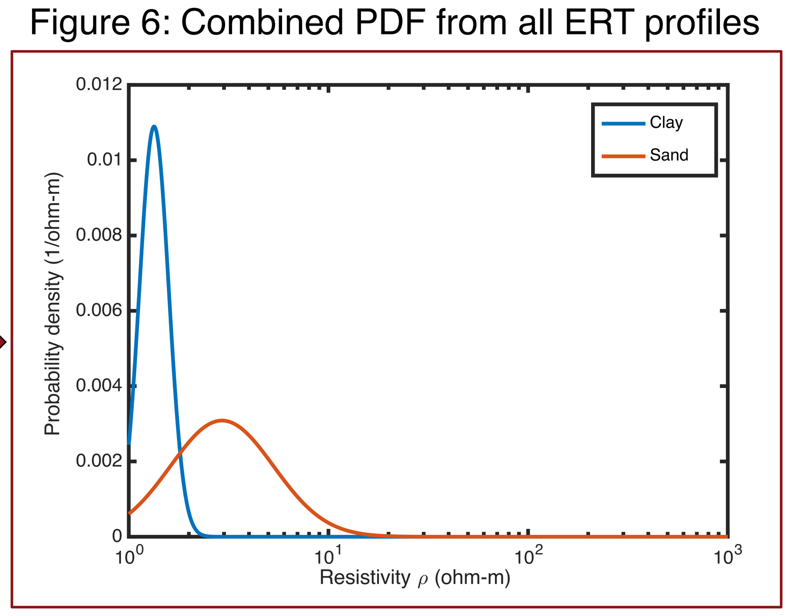


### 3. Simulation-based lithology variation

Workflow:
1) Lithology was simulated based on the 3D variogram of borehole data at the site, using sequential indicator simulation (SISIM), a two-point geostatistical simulation.
2) In the simulated grid, lithology voxels corresponding to the locations of ERT profiles were extracted, and the ratio of clay:sand was taken.
3) Five new grids were simulated using borehole data and ERT data coded according to the clay:sand ratio from step 2.
4) Steps 1-3 were repeated 20 times.

Figure 7: SISIM grid realization

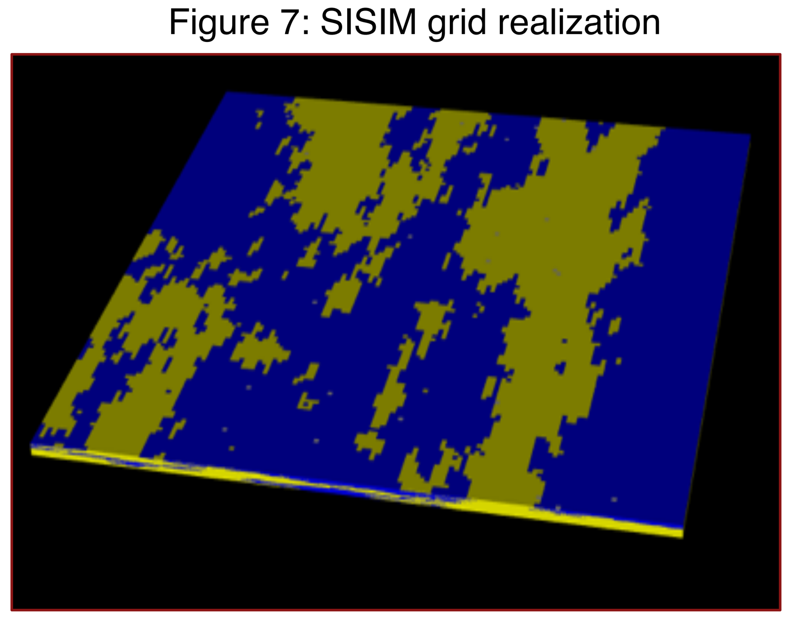

## Discussion

- The search template method does not conform to the sediment resistivities found at the ARR site (Figure 11) or expected values from relationships such as Archie's Law.
- The maximum likelihood estimation and simulated variation methods find plausible resistivity probability distributions given site data.
- The maximum likelihood estimation method is the only method of the three not calibrated to borehole lithology.
- The transformation methods described here can be applied to many different geophysical methods.

## References


- Bowling, J.C., Rodriguez, A. B., Harry, D. L., & Zheng, C. (2005). Delineating alluvial aquifer heterogeneity using resistivity and GPR data. *Ground Water*.
- Caers, J., Srinivasan, S., & Journel, A.G. (2000). Geostatistical Quantification of Geological Information for a Fluvial-Type North Sea Reservoir.
- Hermans, T., Nguyen, F., & Caers, J. (2015). Uncertainty in training image-based inversion of hydraulic head data constrained to ERT data: Workflow and case study. *Water Resources Research*, *51*(7), 5332–5352.
- Larsen, A. L., Ulvmoen, M., Omre, H., & Buland, A. (2006). Bayesian lithology/fluid prediction and simulation on the basis of a Markov-chain prior model.
- Parsekian, A.D., Regnery, J., Wing, A.D., Knight, R., & Drewes, J. E. (2014). Geophysical and Hydrochemical Identification of Flow Paths with Implications for Water Quality at an ARR Site. *Groundwater Monitoring and Remediation*, *34*(3), 105–116.
- Sandberg, S. K., Slater, L. D., & Versteeg, R. (2002). An integrated geophysical investigation of the hydrogeology of an anisotropic unconfined aquifer. *Journal of Hydrology*.


## Results

Figure 8: Conditional probability from search template

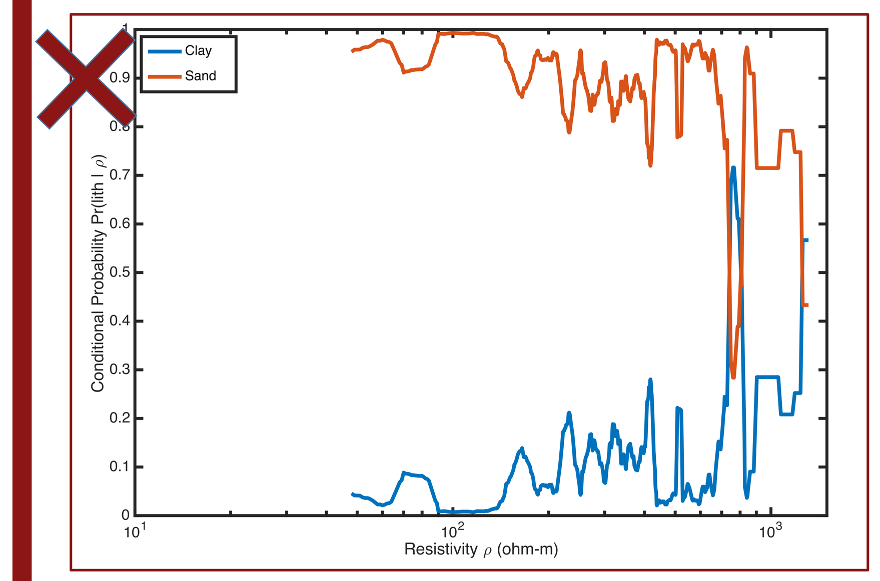


In this case, the search template dramatically skews the empirical probability distribution for a few reasons, including:
- The population of sand dominates that of clay in most wells (Figure 4)
- Small amounts of borehole clay may distort the empirical distribution (see around 750 ohm-m).

Figure 9: Conditional probability from maximum likelihood estimation

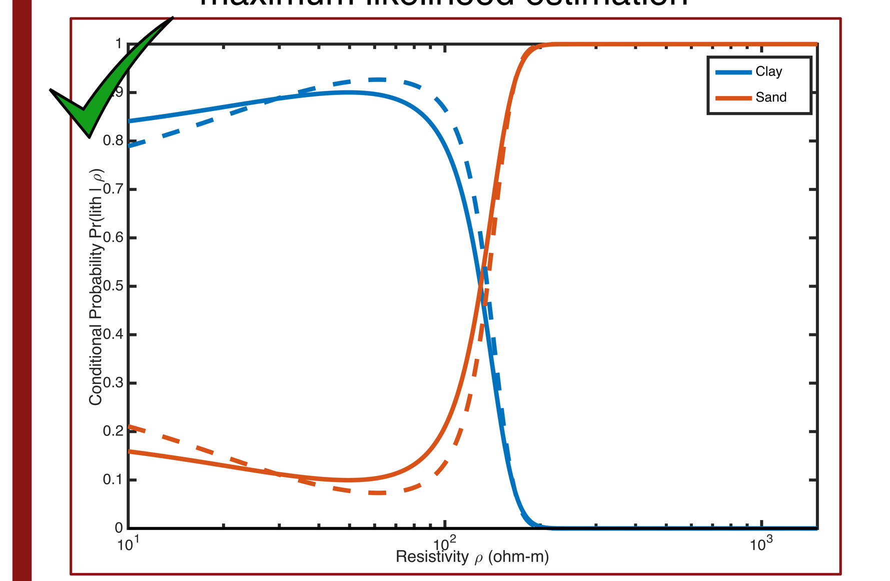


This distribution behaves more conventionally than that created from the search template. High uncertainty (standard deviation in this case) of the sand/gravel facies (Figure 6) disallows the clay facies from ever reaching P=1.

The dashed graph shows the result of the maximum likelihood procedure, fitting one bimodal distribution to the histogram of *all* resistivity measurements in the ARR site.

Figure 10: Conditional probability from simulated lithology variation

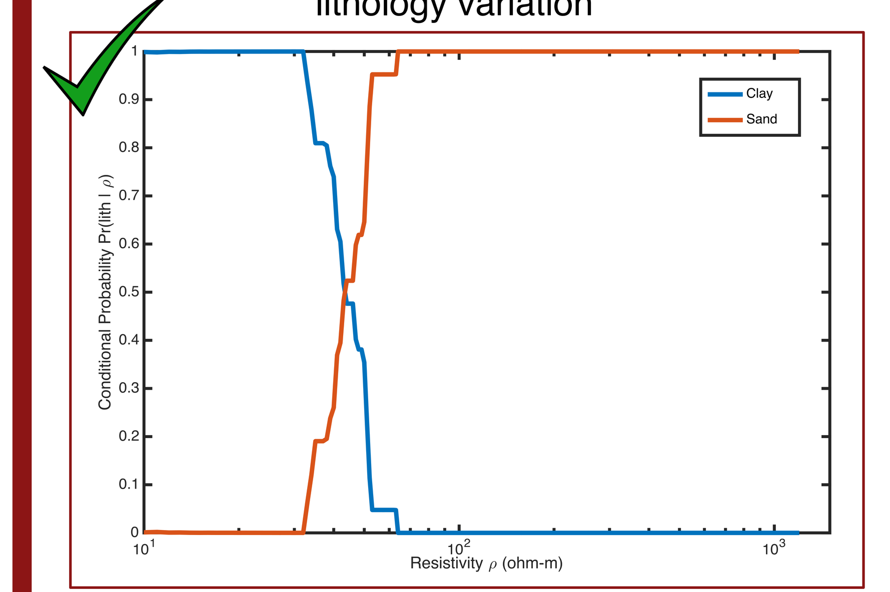


Similar to the probability distribution produced by the maximum likelihood method, this distribution displays a more likely resistivity relationship between sands/gravels and clays/silts.

With an increase in simulations, the distributions will become smoother and change slightly.

Figure 11: Field measurements of resistivity from the ARR site (after Parsekian et al., 2014)

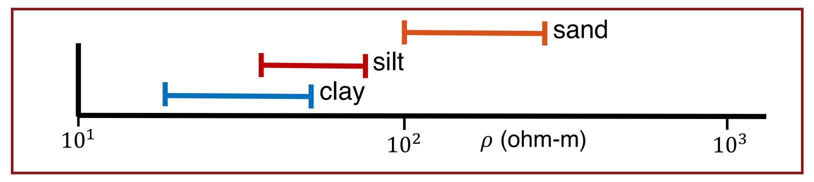


Legend
Clay/slit
Sand/gravel

## Future work

Figure 12: Fluvial training image

Figure 13: MPS lithology realization

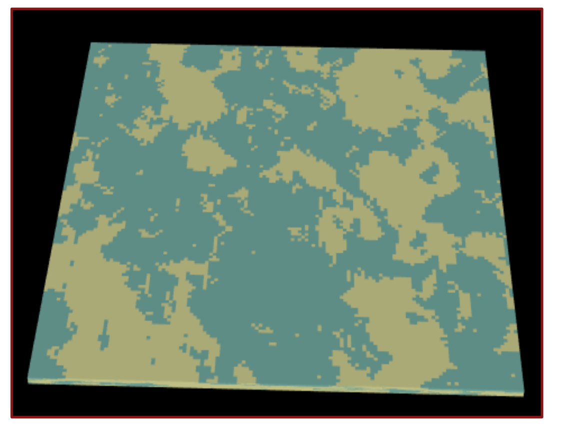

We are incorporating the probabilistic results from this work into multiple point geostatistical (MPS) simulations (Figure 13), which will inform flow simulations. These simulations utilize training images and soft data (Figure 12).